Three-Dimensional GaN-Ga_2O_3 Core Shell Structure Revealed by X-Ray Diffraction Microscopy

Jianwei Miao,[1] Chien-Chun Chen,[2] Changyong Song,[1] Yoshinori Nishino,[3] Yoshiki Kohmura,[3] Tetsuya Ishikawa,[3] Damien Ramunno-Johnson,[1] Ting-Kuo Lee,[2] and Subhash H. Risbud[4]

[1]*Department of Physics and Astronomy and California NanoSystems Institute, University of California, Los Angeles, California 90095, USA*

[2]*Institute of Physics, Academia Sinica, Nankang, Taipei, 11529, Taiwan*

[3]*SPring-8/RIKEN, 1-1-1, Kouto, Mikazuki, Sayo-gun, Hyogo 679-5198, Japan*

[4]*Department of Chemical Engineering and Materials Science, University of California, Davis, California 95616, USA*

(Received 9 July 2006; published 21 November 2006)

In combination of direct phase retrieval of coherent x-ray diffraction patterns with a novel tomographic reconstruction algorithm, we, for the first time, carried out quantitative 3D imaging of a heat-treated GaN particle with each voxel corresponding to $17 \times 17 \times 17$ nm^3. We observed the platelet structure of GaN and the formation of small islands on the surface of the platelets, and successfully captured the internal GaN-Ga_2O_3 core shell structure in three dimensions. This work opens the door for nondestructive and quantitative imaging of 3D morphology and 3D internal structure of a wide range of materials at the nanometer scale resolution that are amorphous or possess only short-range atomic organization.

DOI: 10.1103/PhysRevLett.97.215503 PACS numbers: 61.10.Nz, 42.30.Rx, 42.30.Wb, 61.46.−w

Since Robert Hooke built a compound light microscope based on a three-lens conformation in 1655, lens-based microscopy (such as light, phase-contrast, fluorescence, confocal, and electron microscopy) has played an indispensable role in the evolution of modern sciences and technologies. Because x rays have much shorter wavelengths than visible light and a longer penetration depth than electrons, scientists have long dreamed of atomic-resolution x-ray microscopes that could visualize the arrangement and dynamics of atoms in three dimensions. X rays, however, are much more difficult to focus than electrons. By using x-ray optics, the smallest focal spot currently attainable is ~30 nm for hard x rays [1] and ~15 nm for soft x rays [2]. Furthermore, when the focal spot of soft x rays reaches 15 nm, the depth of focus becomes less than 0.5 μm [3], which limits the thickness of the sample under investigation. In combination of coherent x-ray scattering with a method of direct phase recovery called oversampling, a novel form of lensless microscopy (i.e., x-ray diffraction microscopy), has recently been developed for imaging nanocrystals and noncrystalline specimens [4–11]. The extension from two to three dimensions has also been pursued, which is based upon direct phase retrieval of a 3D diffraction pattern interpolated from a limited number of 2D patterns [12,13]. However, since the diffraction intensity varies at least 5–7 orders from high to low resolution, reciprocal-space interpolation introduces artifacts in the assembled 3D diffraction pattern [14]. The problem becomes even more severe for characterizing structure at the nanometer resolution, as more high-resolution data points need to be interpolated. Here, we report a new scheme for 3D x-ray diffraction microscopy through a combination of (i) *ab initio* phase retrieval of 2D coherent diffraction patterns with a guided hybrid input-output algorithm and (ii) 3D image reconstruction with equally sloped tomography [15,16]. The novelty of our x-ray microscope method is contained in the precision and reliability of both image reconstruction algorithms, and these innovations have allowed us to perform nondestructive and quantitative 3D characterization of materials at the nanometer scale resolution.

We have investigated heat-treated GaN quantum dot particles on which Ga-oxide layers have formed due to heat treatment. The nitride semiconductor was chosen as an example of a group of wide band gap III-V nitride semiconductors that have broad application in electronic and optical device such as blue/green lasers and flat panel displays [17,18]. The GaN quantum dot particles were commercially obtained from Atomergic Chemicals Corp. and heat treated in a flowing stream of pure N_2 gas (flow

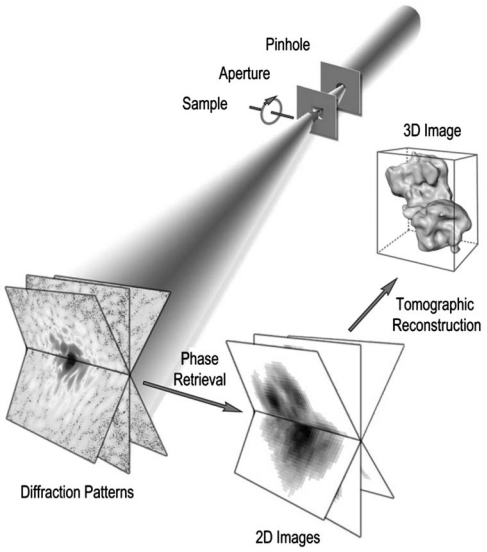

FIG. 1. Schematic layout of the 3D x-ray diffraction microscope, combining *ab initio* phase recovery with tomographic image reconstruction.

rate of 100 ml/min) at several temperatures. The nitrogen atmosphere created an environment with a very low partial pressure of oxygen thus oxidizing the GaN particles at a controllable rate and forming a thin shell of Ga oxide on the GaN core. The nitrogen treated samples, when examined by routine x-ray diffraction, showed characteristic peaks at 31.719° (GaN) and at 35.208° (β-Ga_2O_3) [19]. The particular sample chosen for the 3D study was heated at 900 °C for 24 h. The particles were suspended in ethanol and deposited on 30 nm thick Si_3N_4 membranes. The well-isolated and micron-sized particles were selected by a light microscope and used for the coherent x-ray diffraction.

Our x-ray diffraction microscope, shown in Fig. 1, used a 3rd generation synchrotron undulator at SPring-8 with 5 keV x rays. The temporal coherence of the beamline was $\sim$1.86 μm, and the vertical and horizontal spatial coherence length were $\sim$110 μm and $\sim$30 μm at the sample position. To reduce the illumination size, a 20 μm pinhole was placed in front of the sample. Between the pinhole and the sample was mounted a square silicon aperture with tapered edges, which was used to eliminate the parasitic scattering from the pinhole. The sample was mounted on a rotary stage for acquiring 3D data sets. The coherent x-ray diffraction patterns were recorded on a liquid-nitrogen cooled CCD detector. A beam stop was placed just in front of the detector to block the direct beam. The distance between the sample and the detector was adjustable so that the central missing data due to the beam stop was confined within the centrospeckle [20].

We have obtained 27 coherent x-ray diffraction patterns from a single GaN quantum dot particle with the tilt range of $-69.4°$ to $+69.4°$. The data in the range of $\pm 20.6°$ were not accessible due to the interference between the Si frame and the incident x-ray beam. To enhance the signal to noise ratio, we accumulated $\sim$1500 data sets and merged them into a 2D diffraction pattern at a given tilt angle. The total exposure time for each diffraction pattern is around 12.6 min. To carry out 3D reconstruction, we first inverted each coherent x-ray diffraction pattern to a 2D image. Since there are 27 2D diffraction patterns and any error in each 2D image reconstruction will propagate to the final 3D image, a precise and reliable phase retrieval algorithm is critical to our method. Based on the previous work [21,22], we developed a guided hybrid input-output algorithm (GHIO) for *ab initio* phase retrieval. GHIO started with 16 independent reconstructions on each 2D x-ray diffraction pattern, in which different random phase sets were used as the initial inputs. Each reconstruction iterated back and forth between real and reciprocal space. In real space, the electron density outside a support and the negative density inside the support were slowly pushed close to zero where the support is a boundary somewhat larger than the sample envelope. In reciprocal space, the experimental Fourier magnitude remained unchanged and only the phases were updated. After 2000 iterations, we obtained 16 images (defined as the 0th generation). An R factor for each of the 16 images was calculated by

$$R = \frac{\sum_{k_x,k_y} ||F_{\mathrm{exp}}(k_x, k_y)| - \alpha |F_{\mathrm{cal}}(k_x, k_y)||}{\sum_{k_x,k_y} |F_{\mathrm{exp}}(k_x, k_y)|}, \qquad (1)$$

where $|F_{\mathrm{exp}}(k_x, k_y)|$ and $|F_{\mathrm{cal}}(k_x, k_y)|$ represent the experimental and calculated Fourier magnitude, α a scaling factor, and k_x, k_y the coordinates in reciprocal space. A seed image was chosen corresponding to the smallest R factor. After aligning the 16 images (ρ^i_{old}) to the seed (ρ_{seed}), a new set of 16 images was obtained by

$$\rho^i_{\mathrm{new}} = \sqrt{\rho_{\mathrm{seed}} \rho^i_{\mathrm{old}}}, \qquad i = 1, 2, \cdots, 16, \qquad (2)$$

which were used as the initial inputs for the next generation. This step was to merge the best image in the current generation with each of the 16 images so that the "favorable gene" (i.e., smaller R factor) would be passed to the succeeding generations. Furthermore, after the multiplication of the two independent images, the density fluctuation in the new image was significantly reduced. We repeated the procedure for each generation and, usually after 9 generations, the 16 reconstructed images became virtually identical. While requiring more computational power, GHIO is precise and reliable in *ab initio* phase retrieval of coherent x-ray diffraction patterns. The details on GHIO will be described in a follow-up paper. We applied GHIO to each of the coherent x-ray diffraction patterns and obtained 27 2D images. After being aligned

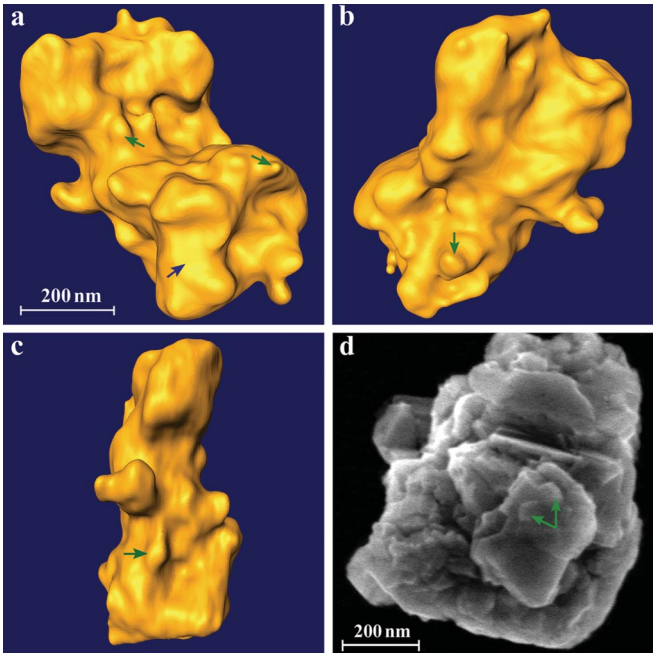

FIG. 2 (color). Isosurface rendering of a reconstructed 3D GaN quantum dot particle, showing (a) the front view, (b) the back, and (c) the side view. (d) SEM image of a different GaN nanoparticle. The GaN quantum dot particles were heat-treated under N_2 at 900 °C for 24 h. The size of the platelet indicated by a blue arrow in (a) is $\sim 260 \times 120 \times 50$ nm^3. The formation of small islands on the surface of the particles is clearly visible (some of them are labeled with green arrows).

with the tilt axis, the 27 2D images were used to reconstruct a 3D image based on equally sloped tomography [15,16]. To check the quality of the reconstructed 3D image, we projected it back to obtain 27 2D images, which were consistent to the original ones.

By using the two reliable algorithms, we have obtained a quantitative 3D image of the GaN quantum dot particle. Figure 2 shows an isosurface rendering of the reconstructed 3D image, where Figs. 2(a)–2(c) represent the front, back, and side view of the particle. A distinctive feature of the particle is the plateletlike structure. The particle consists of a few platelets at different orientations. We measured the size of a single platelet indicated by a blue arrow in Fig. 2(a), which is $\sim 260 \times 120 \times 50$ nm. By examining the 3D surface morphology, we observed the formation of small islands with varied size on the surface of the particle (labeled with green arrows in Fig. 2), which is a result of the surface oxidation of GaN platelets after the heat treatment. While the platelet structure and the formation of small islands on the surface are visible in the scanning electron microscope image shown in Fig. 2(d) (not the same particle), the 3D x-ray images clearly provide more complete and quantitative morphological views of the structure [23].

In order to quantitatively visualize the 3D internal structure, we sectioned the particle slice by slice with each corresponding to 17 nm thick. Figure 3 shows a set of 20 slices between $z = 0$ and $z = 340$ nm, where the platelet structure of GaN is clearly visible (see, e.g., $z = 255$–323 nm). The colors in the slices represent the different electron density with red the high density, yellow the medium density, and blue the low density. Figure 3 shows that the high density, concentrated near the center of the platelets, is surrounded by the low density. It is reasonable to conclude that the low electron density is from the β-Ga_2O_3 regions of the particle while the high electron density is from the GaN. During the GaN surface oxidation process, small islandlike features of β-Ga_2O_3 formed on the surface of the platelets, which likely have lower quality of crystallinity than the GaN cores and give rise to the low electron density. The observation provides direct evidence of the existence of 3D GaN-Ga_2O_3 core shell structure in heat-treated GaN platelets, which is not readily visualized by electron microscopy or conventional x-ray diffraction [19].

Photoluminescence spectra of the GaN with β-Ga_2O_3 layers showed an enhancement of the near band-edge emission and suppression of yellow emission [19], which can be explained by using Fig. 3. The β-Ga_2O_3 layer is the passivating layer that must decrease the concentration of GaN surface dangling bonds. As the β-Ga_2O_3 layers form from the surface toward the center of GaN, the size of the GaN cores gets smaller and smaller (see the electron density in red in Fig. 3) and eventually reaches dimensions comparable to or less than the exciton Bohr diameter (quantum confinement effect). Our quantitative 3D images will provide an effective feedback loop in the synthesis and processing of quantum dots with application as light emitting materials for blue and UV-lasers [17,18]. In these quantum dot based devices, strong quantum confinement effects arise from carriers that are confined in all three spatial dimensions. This is because increased oscillator strengths and large, resonant third order nonlinearities are predicted for quantum dots. Furthermore, quantitative 3D x-ray diffraction microscopy can be a very valuable tool to address some important issues in quantum dot semiconductor materials processing, e.g., imaging the morphology of dots with different lattices, imaging thin interfacial layers at the substrate-quantum dot interface, and locating defects in and on the surface of nanostructure.

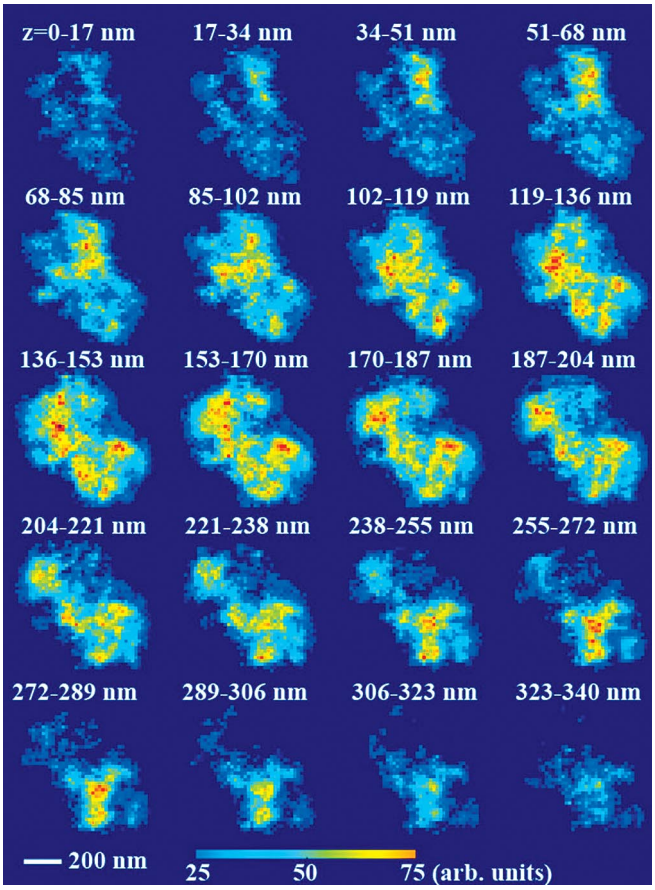

FIG. 3 (color). 3D internal structure of the GaN quantum dot particle, where the z axis is perpendicular to the front view [Fig. 2(a)] and points outward. The 3D GaN-Ga_2O_3 core shell structure is clearly visible where the low electron density corresponds to β-Ga_2O_3 and the high density corresponds to the GaN cores.

In combination of *ab initio* phase retrieval of coherent x-ray diffraction patterns with equally sloped tomographic reconstruction, we carried out nondestructive and quantitative 3D imaging of a heat-treated GaN quantum dot particle at the nanometer scale level. We observed the platelet structure of the GaN quantum dot particle and the formation of small islands on the surface of the particle. By examining the 3D internal structure of the GaN particles, we successfully captured the GaN-Ga_2O_3 core shell structure in three dimensions with each voxel correspond-

ing to $17 \times 17 \times 17$ nm^3. While the current resolution is limited by the detector size and coherent x-ray flux, the ultimate resolution is only set by the x-ray wavelengths. Unlike transmission electron microscopy, the x-ray imaging technique does not require destructive sample preparation and can study materials with varied thickness in three dimensions. The present work hence opens the door for comprehensive, nondestructive and quantitative 3D imaging of a wide range of samples including porous materials, semiconductors, quantum dots and wires, inorganic nanostructures, granular materials, biomaterials, and cellular structure. As more brilliant x-ray sources such as x-ray free electron lasers [24] and energy recovery linacs [25] are under rapid development worldwide, the combination of these sources with x-ray diffraction microscopy will open up a new horizon for 3D imaging of noncrystalline materials, nanocrystals, and disordered solids at the nanometer or even near-atomic level.

We thank H. Jiang for valuable discussions and help with figures. The experiment was performed on beam line BL29XUL at SPring-8, which was funded by RIKEN. This work was supported by the U. S. Department of Energy, Office of Basic Energy Sciences (No. DE-FG02-06ER46276) and the U.S. National Science Foundation, Division of Materials Research (No. DMR-0520894).

[1] H. C. Kang, J. Maser, G. B. Stephenson, C. Liu, R. Conley, A. T. Macrander, and S. Vogt, Phys. Rev. Lett. **96**, 127401 (2006).
[2] W. Chao, B. D. Harteneck, J. A. Liddle, E. H. Anderson, and D. T. Attwood, Nature (London) **435**, 1210 (2005).
[3] C. Jacobsen, J. Kirz, and S. Williams, Ultramicroscopy **47**, 55 (1992).
[4] J. Miao, P. Charalambous, J. Kirz, and D. Sayre, Nature (London) **400**, 342 (1999).
[5] I. K. Robinson, I. A. Vartanyants, G. J. Williams, M. A. Pfeifer, and J. A. Pitney, Phys. Rev. Lett. **87**, 195505 (2001).
[6] S. Marchesini, H. He, H. N. Chapman, S. P. Hau-Riege, A. Noy, M. R. Howells, U. Weierstall, and J. C. H. Spence, Phys. Rev. B **68**, 140101 (2003).
[7] K. A. Nugent, A. G. Peele, H. N. Chapman, and A. P. Mancuso, Phys. Rev. Lett. **91**, 203902 (2003).
[8] J. Miao, K. O. Hodgson, T. Ishikawa, C. A. Larabell, M. A. LeGros, and Y. Nishino, Proc. Natl. Acad. Sci. U.S.A. **100**, 110 (2003).
[9] X. Xiao and Q. Shen, Phys. Rev. B **72**, 033103 (2005).
[10] D. Shapiro, P. Thibault, T. Beetz, V. Elser, M. Howells, C. Jacobsen, J. Kirz, E. Lima, H. Miao, A. M. Neiman, and D. Sayre, Proc. Natl. Acad. Sci. U.S.A. **102**, 15 343 (2005).
[11] H. M. Quiney, A. G. Peele, Z. Cai, D. Paterson, and K. A. Nugent, Nature Phys. **2**, 101 (2006).
[12] J. Miao, T. Ishikawa, B. Johnson, E. H. Anderson, B. Lai, and K. O. Hodgson, Phys. Rev. Lett. **89**, 088303 (2002).
[13] H. N. Chapman, A. Barty, S. Marchesini, A. Noy, S. P. Hau-Riege, C. Cui, M. R. Howells, R. Rosen, H. He, J. C. H. Spence, U. Weierstall, T. Beetz, C. Jacobsen, and D. Shapiro, J. Opt. Soc. Am. A **23**, 1179 (2006).
[14] The 3D imaging experiment that Robinson and collaborators have recently demonstrated does not require reciprocal-space interpolation [M. A. Pfeifer, G. J. Williams, I. A. Vartanyants, R. Harder, and I. K. Robinson, Nature (London) **442**, 63 (2006)] as it provides quantitative 3D mapping of lattice strain instead of 3D electron density.
[15] Conventional tomography reconstructs a 3D object from a set of equally angled projections. Since the set of projections are in polar coordinates and the object in Cartesian coordinates, interpolation has to be used in the reconstruction process, which introduces artifacts in the reconstructed 3D object, especially when there are a limited number of projections. Equally sloped tomography has recently been developed to reduce the reconstruction artifacts [16]. Unlike conventional tomography, the new approach makes use of a set of equally sloped projections. Since the projections are equally sloped instead of equally angled, it is called pseudopolar instead of polar coordinates. By applying the Fourier transform to each projection, a set of Fourier slices in pseudopolar coordinates are calculated. To reconstruct a 3D image from the Fourier slices, the pseudopolar fast Fourier transform is used to iterate back and forth between real (Cartesian coordinates) and reciprocal space (pseudopolar coordinates), where the pseudopolar fast Fourier transform is a new variation of the fast Fourier transform [A. Averbuch, R. R. Coifman, D. L. Donoho, M. Elad, and M. Israeli, Appl. Comput. Harmon. Anal. **21**, 145 (2006)]. In real space, the electron density outside the sample boundary is slowly pushed close to zero. In reciprocal space, the known Fourier slices (i.e., both amplitude and phases) remain unchanged and the missing slices are kept floating in each iteration. The reconstruction process is very consistent, and usually after about a hundred iterations, a 3D object can be obtained. The details on equally sloped tomography can be found elsewhere [16].
[16] J. Miao, F. Förster, and O. Levi, Phys. Rev. B **72**, 052103 (2005).
[17] S. Nakamura, Science **281**, 956 (1998).
[18] *Quantum Semiconductor Devices and Technologies*, edited by T. P. Pearsall (Kluwer, Dordrecht, 2000).
[19] J. Tong and S. H. Risbud, J. Solid State Chem. **177**, 3568 (2004).
[20] J. Miao, Y. Nishino, Y. Kohmura, B. Johnson, C. Song, S. H. Risbud, and T. Ishikawa, Phys. Rev. Lett. **95**, 085503 (2005).
[21] J. R. Fienup, Opt. Lett. **3**, 27 (1978).
[22] C. I. Chou and T. K. Lee, Acta Crystallogr. Sect. A **58**, 42 (2002).
[23] See EPAPS Document No. E-PRLTAO-97-036647 for a 3D movie of the GaN quantum dot particle. For more information on EPAPS, see http://www.aip.org/pubservs/epaps.html.
[24] C. Pellegrini and J. Stöhr, Nucl. Instrum. Methods Phys. Res., Sect. A **500**, 33 (2003).
[25] D. H. Bilderback, I. V. Bazarov, K. Finkelstein, S. M. Gruner, H. S. Padamsee, C. K. Sinclair, Q. Shen, R. Talman, M. Tigner, G. A. Krafft, and L. Merminga, J. Synchrotron Radiat. **10**, 346 (2003).